UDC 612.115 doi: https://doi.org/10.15407/ubj97.01.062

DEVELOPMENT OF POLYMER SYSTEMS CAPABLE OF COUNTERACTING SURFACE-INDUCED FIBRILLOGENESIS

A. HANSEN[1], A. SLOUTSKI[1], R. WONG[1], Y. FANG[1],
L. STOTCHEL[2], C. SADASIVAN[3], M. RAFAILOVICH1

[1]Department of Materials Science and Engineering,
Stony Brook University, Stony Brook, New York, USA;
[2]Hebrew Academy of Nassau County, Uniondale, New York, USA;
[3]Department of Neurosurgery, Stony Brook University,
Stony Brook, New York, USA;
✉e-mail: adam.hansen@stonybrook.edu

Received: 06 November 2024; **Revised:** 27 January 2025; **Accepted:** 21 February 2025

It is known that the use of medical devices having polymer surfaces exposed to blood flow often leads to thrombogenesis. The mechanism of thrombus formation depends, in part, on the hydrophobic/hydrophilic nature and adhesive properties of the surface, on which spontaneously initiated fibrillogenesis can occur in the absence of thrombin. In this work, the connection between the "Berg limit" and the ability of polymer surfaces to aggregate fibrinogen into fiber structures was investigated using two unique systems. Polystyrene (PS), a well-characterized, stable polymer, was first tested because of its ability to readily impart hydrophilicity using UV-ozone without additional additives. However, in order to explore a biodegradable polymer with greater physiological relevance, the focus was switched to polyvinyl alcohol (PVA). To improve the mechanical properties and increase the hydrophilicity of PVA, a chemical approach was used with the addition of the clay functionalized with resorcinol diphenyl phosphate (RDP). Observations for the two different systems indicated that fibrinogen absorption undergoes a transition through the Berg limits, regardless of a physical or chemical approach, and that there was a significant reduction in surface fibrillogenesis with contact angles below this threshold. Finally, HUVEC cell adhesion to the surface of PVA-RDP with no negative effect on proliferation and endothelialization capability was demonstrated. A guideline is proposed for designing non-thrombogenic materials by rendering the surface hydrophilic. This phenomenon could be applied to engineering polymers more applicable to biomedical purposes.

Keywords: fibrinogen absorption, fiber formations, polymer surfaces, Berg limit, thrombogenicity, HUVEC cells.

The blood clotting process is crucial for preventing excessive bleeding by forming stable clots through the action of platelets and coagulation factors [1]. In the case of injury, a signaling cascade is initiated, and the final steps occur when thrombin is released. This cleaves the fibrinopeptides of the main protein in blood, fibrinogen (Fg), releasing the αC chains, which in turn initiates fibrillogenesis [2]. While in the presence of flowing blood, this process is often incomplete and results in the formation of small soluble aggregates, classified as protofibrils coated with fibrinogen and other blood proteins, which allows them to circulate. These complexes are also known as soluble fibrin and form a stable component in the bloodstream. When fibrinogen is isolated, there is a significant component of soluble fibrin, which has been shown to be the primary contributor to fibrillogenesis initiated on surfaces [3, 4]. Hence, surface fiber formation occurs with the adsorption of fibrinogen, allowing the incorporation of soluble fibrin, which leads to the growth of large surface fibers (Fig. 1, *A*). Such fibers have been shown to provide functional domains for platelet adhesion, activation, and agglomeration [5-7].

The study of surface interactions with blood proteins–particularly fibrinogen–has gained significant importance [8, 9]. The development of medical devices featuring polymeric surfaces exposed to blood flow is often known to result in thrombosis as well, without the presence of thrombin. While multiple factors have been proposed, it has been recently shown that interaction of the device surface with fibrinogen can result in misfolding of the molecules, and formation of surface-initiated clots if the surface possesses hydrophobic attributes [5, 10, 11]. A crucial parameter to consider when dealing with biomacromolecules surface adhesion studies is the “Berg limit” [12]. The “Berg limit” is a range of contact angles, 50-70 degrees, that is defined as the threshold at which surfaces transition to exhibit notable adhesive properties in aqueous environments. Surfaces with contact angles below this threshold generally repel biomolecules, while those above show significantly enhanced attraction and adhesion. The attraction or repulsion of biomolecules also positions a surface to support or reject cell adhesion, which is particularly important for materials requiring endothelialization for proper integration. One such material showing promise for applications in artificial blood vessels is polyvinyl alcohol (PVA), whose mechanical properties are similar to those of vascular tissue. Hence, this polymer can be sutured directly onto existing vasculature and has similar values of the burst pressure. However, the hydrophilic nature of PVA makes it challenging to support cell adhesion, which in turn would prevent further endothelialization [13-15].

In this manuscript, we explore the conditions of the surface which lead to the misfolding of fibrinogen molecules. We show that using contact angle goniometry we can establish a functional definition of the degree of hydrophobicity where surface fibrillogenesis is spontaneously initiated in the absence of thrombin. Two approaches to producing surfaces of varying degrees of hydrophobicity are explored; ultraviolet (UV)-ozone irradiation of the host polymers, which exposes multiple functional groups [16, 17], and inclusion of clay nanoparticles functionalized with resorcinol bis (diphenyl phosphate) (RDP), which can change hydrophobicity without modification of the host polymer matrix with a non-toxic chemical addition [18-20]. Furthermore, the insertion of devices in the bloodstream assumes eventual endothelialization and incorporation into the vascular system. Hence, the impact of surface hydrophobicity modifications on endothelial cell adhesion and proliferation was also explored with the goal of providing guidelines for the design of materials featuring properties conducive to both non-thrombogenicity and cytocompatibility.

Materials and Methods

Surface preparation. Silicon wafers, cut into squares of length and width each 1 cm, were used as the underlying substrate for spun cast thin films of approximately 350 nm in thickness. The polystyrene (PS) (Mw = 311,100) was dissolved using a toluene solvent to create a polymer solution with a concentration of 15 mg/ml. The PVA (Mw = 85,000-124,000) was dissolved using a deionized (DI) water solvent with a concentration of 20 mg/ml. These solutions were then used to coat onto cleaned silicon wafers. Wafers were washed in piranha solution to etch and create oxide layers for more uniform thin films. Clay functionalized with RDP (RDP-clay) was prepared by manually mixing 40g of Cloisite Na^+ clay and 10 g of RDP for 3 min then placing in a Thinky Mixer ARE-250 at 2000 RPMs for 10 min. Samples were ground three times in a mortar to create finer particles and then annealed overnight at 60°C to remove moisture. For incorporation of RDP-clay into the spun cast polymer matrices, various concentrations of RDP-clay were annealed at 160°C overnight, then added into the dissolved PVA solutions, mixed at 80-90°C for 2 h, and sonicated in a heat bath for 30 min prior to spin casting. The settings used for spin casting thin films were 2500 rotations per minute (RPMs), accelerated at 1000 RPMs/sec, for 30 sec each. Once coated, PS and PVA/RDP-clay films were annealed at 180°C and 160°C respectively, for approximately 24 h for sterilization, relaxation of polymer chains, and removal of remaining chemicals from the surface. For PS films treated with UV ozone, a PSD Pro Series Digital UV-Ozone System from Novascan was used for varying durations post-annealing.

Fibrinogen deposition. Fibrinogen, depleted of plasminogen, von Willebrand factor, and fibronectin and purified from human plasma were obtained from Enzyme Research (South Bend, IN USA). The fibrinogen was dissolved in Dulbecco’s Phosphate Buffered Saline (PBS) to prepare a concentration of 4 mg/ml to be utilized for fibrinogen plating and imaging of individual fibrin fibers. Films were incubated by covering the surface with drops of approximately 300 μl of fibrinogen solution for exactly 1 h to cover the surface, diluted and washed with PBS, washed three times with DI water to remove any salt from the sample, and then air-dried for imaging.

Analysis of adsorbed fibrinogen. To obtain the high-resolution images of fibrin fibers on the surface, Atomic Force Microscopy (AFM) was performed using a Dimension 3000 in contact mode (height and deflection) at a scan rate of 1 Hz. Scanning images were obtained by utilization of a non-conductive silicon nitride probe from Veeco (NP), with a nominal tip radius of 0.4-0.7 µm and a spring constant of 0.12 N/m. Fiber analysis was done using Nanoscope software from Digital Instruments. Optical images for surface fiber quantification were taken using an Olympus BH-2 microscope.

Surface characterization. Surface images were obtained through AFM microscopy in contact mode (height and friction). Surface roughness measurements were obtained using a Keyence laser microscope, analyzing the topographical variations of the surface at scan sizes of 500 µm and calculating differences in height to be the average roughness. Contact angle measurements were calculated as an average by obtaining three different points on each sample surface using an optical contact angle meter from KSV Instruments. Thickness of the surface was obtained through ellipsometry. FTIR spectra were recorded using a Nicolet iS-50 spectrometer with a resolution of 4 cm-1 by collecting 40 scans for a single spectrum at room temperature at the range of 600-4000 cm^{-1}. The spectra were treated using Origin software.

Cell culture and proliferation. Thin films (sized 1×1 cm) containing 10% PVA and 0, 1, 3, 5, and 10% RDP clay were prepared as substrates for cell proliferation studies as described in the previous sections (N≥5). Thin films were considered sterile after they were annealed overnight at 160°C, and the films were placed into the wells of a sterile 24-well tissue culture plate (Sarstedt, Nümbrecht, Germany). Human umbilical vascular endothelial cells expressing green fluorescent protein (HUVEC-EGFP) were cultured in endothelial growth medium 2 (EGM 2) (Lonza Bioscience, Basel, Switzerland) with media exchanges every other day until 80% confluency. Cells were harvested and plated at a density of 3000 cells/cm^2 into each well of a 24-well plate. Cell proliferation was quantified through Alamar blue assays on days 1, 3, and 5. Before each Alamar blue assay, the wafers were placed into a new 24-well plate so that only the cells on the thin film would be measured. An Alamar blue assay was conducted by forming Alamar blue media which consisted of 90% EGM 2 and 10% Alamar blue (ThermoFisher Scientific, Waltham, MA, USA). Each well received 0.5 ml Alamar blue media and the cells were cultured for 4 h in an incubator (37°C, 5% CO_2). Afterward, 100 µl of Alamar blue media was drawn from each well and placed into the wells of a 96-well plate. A microplate reader was used to measure the absorbance. The Alamar blue media was then aspirated from each well and replaced with 0.5 ml of EGM 2. Statistical analysis was performed using a one-way analysis of variance (ANOVA) test was performed on all cell-work analysis to determine differences in cell growth ($P < 0.05$). Mean and standard deviation are represented in all other work.

Results and Discussion

Determining the critical contact angle for surface-induced polymerization. The initial investigation aimed at testing and determining the surface properties of PS thin films by analyzing several aspects of the polymer with no changes to its chemistry. The goal was to obtain a thin, hydrophobic surface that could be altered through UV-ozone exposure to reduce the water contact angle then study the transition from a thrombogenic to a non-thrombogenic surface, which would require a reduction beyond the Berg limits to be reached and some critical angle to be determined that halts protein adsorption. Once elucidated using the model polymer PS, this phenomenon could be applied to engineering polymers more applicable to biomedical purposes.

Data from Fig. 1 represents the specific properties obtained for the PS surfaces following UV-ozone treatment and fibrinogen incubation, which aimed to increase its hydrophilicity and alter the surface-interaction of fibrinogen. At a water contact angle of about 82°, unaltered control PS surfaces resulted in fibrinogen readily adsorbed to the surface and polymerization into fibrin fibers, which is illustrated in Fig. 2. This means that PS induces surface-initiated thrombogenicity and its hydrophobic properties are sufficient to cause conformational changes of the adsorbed fibrinogen molecules, thereby exposing their αC regions and leading to polymerization. To attempt to eliminate this property, PS surfaces were exposed to UV-ozone irradiation to reduce contact angle and increase hydrophilicity, which should lead to less adsorption and less distortion of fibrinogen and, furthermore, reduced fiber generation. Initial studies tested the effect of UV-ozone duration on PS contact angle measurements and is represented in Fig. 1, *B*, which shows that contact angles decrease linearly as a function

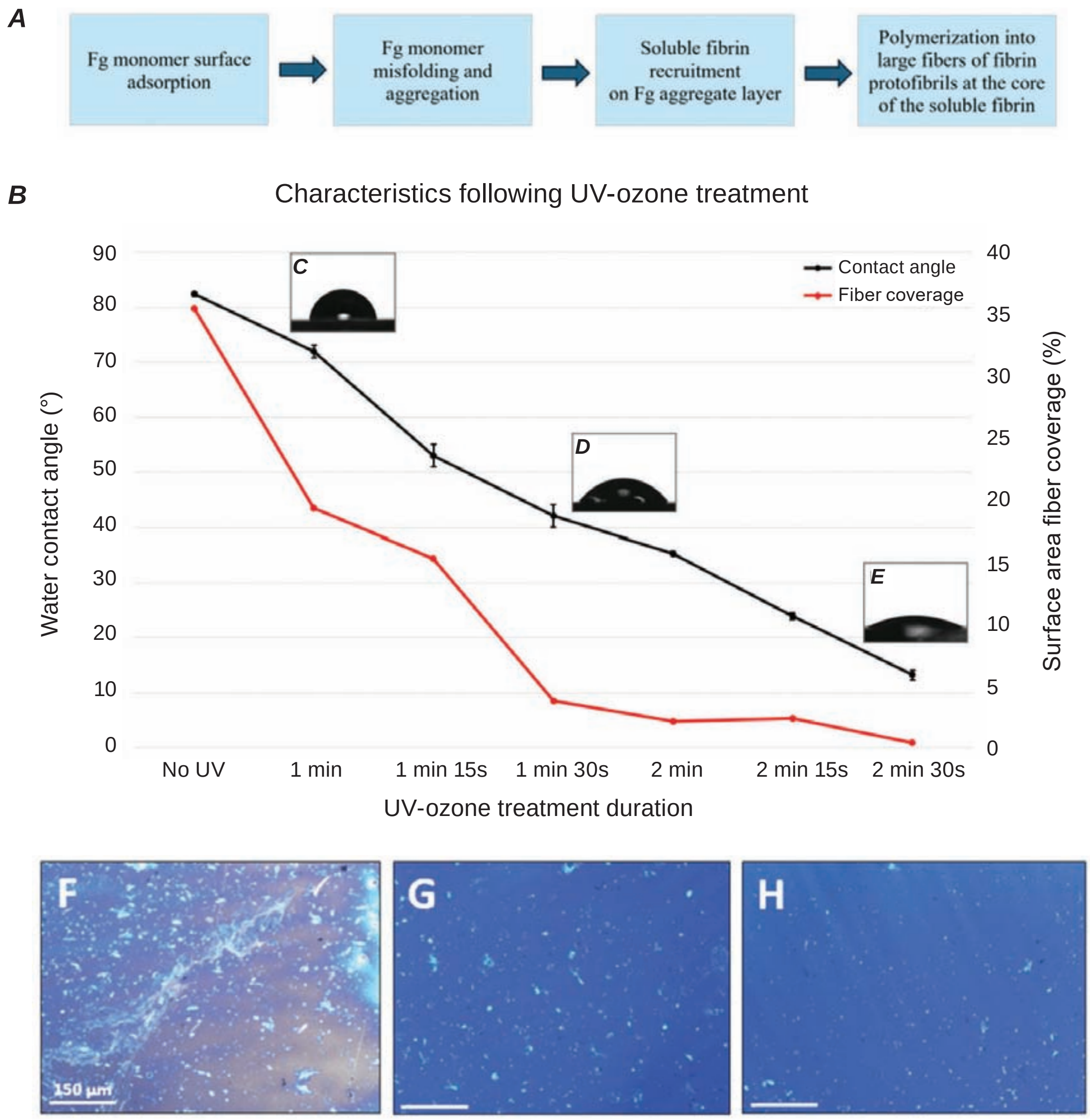

*Fig. 1. Surface fiber formation summary diagram (**A**). Contact angle and fiber coverage studies on PS as a function of the ozone treatment time (**B**). Images highlighting maximum contact angle (**C**) 80°, critical angle (**D**) 40°, and minimum (**E**) 15°. Optical images of coverage with (**F**) control, (**G**) 1 min 30s, and (**H**) 2 min 30s treatment*

of UV-ozone time. From 1 min to 2 min, there was a gradual decrease from about 72° to 35°. The past 2 min treatment led to decreases down to roughly 13°, which was produced at the maximum exposure time of 2 min and 30 sec. This further increased the hydrophilicity of the PS surface significantly. Next, the effectiveness of this increase in wettability of PS on the adsorption of fibrinogen and its tendency to misfold and generate fibers was further investigated. Fibrinogen adsorption and consequential fiber formations on controlled and altered PS surfaces following overnight incubation of 4 mg/ml fibrinogen solutions were analyzed in a variety of ways. The initial characterization is shown in Fig. 1 where optical images were collected and full surface quantification was performed representing the total surface coverage of distinctly formed fibers, excluding small agglomerations of protein, and directly correlating them to water contact angle measurements. As expected, when contact angles decrease, so too does the quantity of surface fiber formations. This can be attributed to the increase in hydrophilicity of the surface, as explained previously. As shown in the graph, from 80° and a fiber surface coverage of around 35% for the control there is a steady linear decrease to about 20% coverage at 72° and 15% coverage at

53°. Furthermore, and most notably, an exponential relationship existed between surface contact angle and fiber coverage when it reached a certain point, which was around 40° to 45°. Here, a steep decline in surface fibers was observed down to a coverage of just 3.85%. This quality remained consistent as the contact angle decreased well below 40° where surface coverage varied at around 1 to 3%. Fig. 1, *C*, *D*, and *E* represent images of contact angle measurements taken on PS at 80°, 40°, and 15°, respectively, which allows for a clear visualization of how wettability is altered from the treatment of UV-ozone. Wettability of a surface has a direct correlation to protein interactions, especially when water readily forms layers and reduces intermolecular hydrogen bonding [20]. Data from Fig. 1, *F*, *G*, and *H* represent images taken from the optical collection used to quantify the surface coverage and help visually depict the differece between high and low contact angles using a large scale. Fig. 1, *F* captures a control sample that received no UV-ozone irradiation with a contact angle of about 80°. The middle of the image contains a massive fiber formation that stretches out of the scope of the image area, which is 800×600 μm^2. Furthermore, almost the entire surface is covered in fibers. This is vastly different from the image in Fig. 1, *G*, representing a contact angle of about 40° after 1.5 min of UV-ozone treatment, where there is a minimal amount of small, scattered fibers on the surface. Fig. 1, *H* depicts the optical image for contact angles under 40° (specifically 24°) where no significant protein visibility is present. This finding further illustrates the effects of the surface Berg limits phenomenon, which suggests the conclusion that fibers have an exceptionally difficult time forming on surfaces with a contact angle below 50° [12] and, hence, it is reasonable to further suggest that fibrinogen adsorption is lower, or that the adsorbed fibrinogen is conformationally different depending on the surface properties. This suggests that only a specific limit exists regarding surface wettability to promote the formation of fibers. These results help establish an aim and direction for designing surface properties in further testing.

Analysis of fiber formations using AFM. To further investigate the fiber formations on PS surfaces as a function of contact angle, we performed AFM imaging to take a closer look at these fibers in detail at the microscale. Data from Fig. 2 represents individual fibers from AFM scans with areas of 50 and 10 μm^2, respectively. Deflection images for highly detailed structure and height images for the characteristics of fibers were obtained. The accompanying maximum height of fiber polymers formed is tabulated in Fig. 2, *I*. Examining the control PS surface (Fig. 2, *A*, *B*), a network of coarse, fully formed fiber structures throughout the whole scope of the image was observed. These fibers reached a maximum height of 195 nm, which was quite significant compared to all other samples. This shows that fibers dynamically formed on the control surface, without disruption due to surface properties. However, significant decreases in fiber polymerization and, thereby, maximum fiber height were observed on all UV-ozone irradiated PS samples. Although the fiber polymers were not fully deterred, 1-min irradiation (Fig. 2, *C*, *D*) produced decreased structure and a less dynamic network with maximum height significantly reduced to about 105 nm. After 1.5-minute irradiation (Fig. 2, *E*, *F*), similar conclusions were observed with even further deductions, now with a maximum height of about 72 nm and far less visible structure and skinny fibers. Finally, after 2-minute irradiation (Fig. 2, *G*, *H*) almost no fiber structure at all exists. Significantly smaller, thinner fibers with a maximum height of roughly 43 nm are observed.

Designing a non-thrombogenic PVA material. Now, that an initial insight into the requirements for surface fibrillogenesis and its connection to Berg limit phenomena was obtained, the next step aimed to exemplify this understanding by utilizing a more appropriate biomaterial application in PVA. However, at a water contact angle of about 50°, PVA is directly on the lower limit of the Berg threshold for protein adsorption. Therefore, to increase effectiveness, the water contact angle should aim to be below this critical angle. To eliminate this property and increase hydrophilicity, PVA surface chemistry was altered through the inclusion of various percentages of RDP-clay into the polymer to create nanocomposite materials. RDP-clay is a substance previously shown to affect surface roughness, which also alters protein adsorption and potentially cell adherence capabilities [21].

Characterization of RDP-clay. RDP-clay was characterized using FTIR analysis (Fig. 3, *A*). The spectrum of the RDP polymer corresponds with previously obtained data [20]. Phosphorus−oxygen double bond stretching (P═O) at ~1300 cm^{-1} and the phosphorus−oxygen single bond stretching (P−O) at ~940 cm^{-1} are visible alongside the sharp carbon oxide (C=O) peak at 1588 cm^{-1}. The unmodified

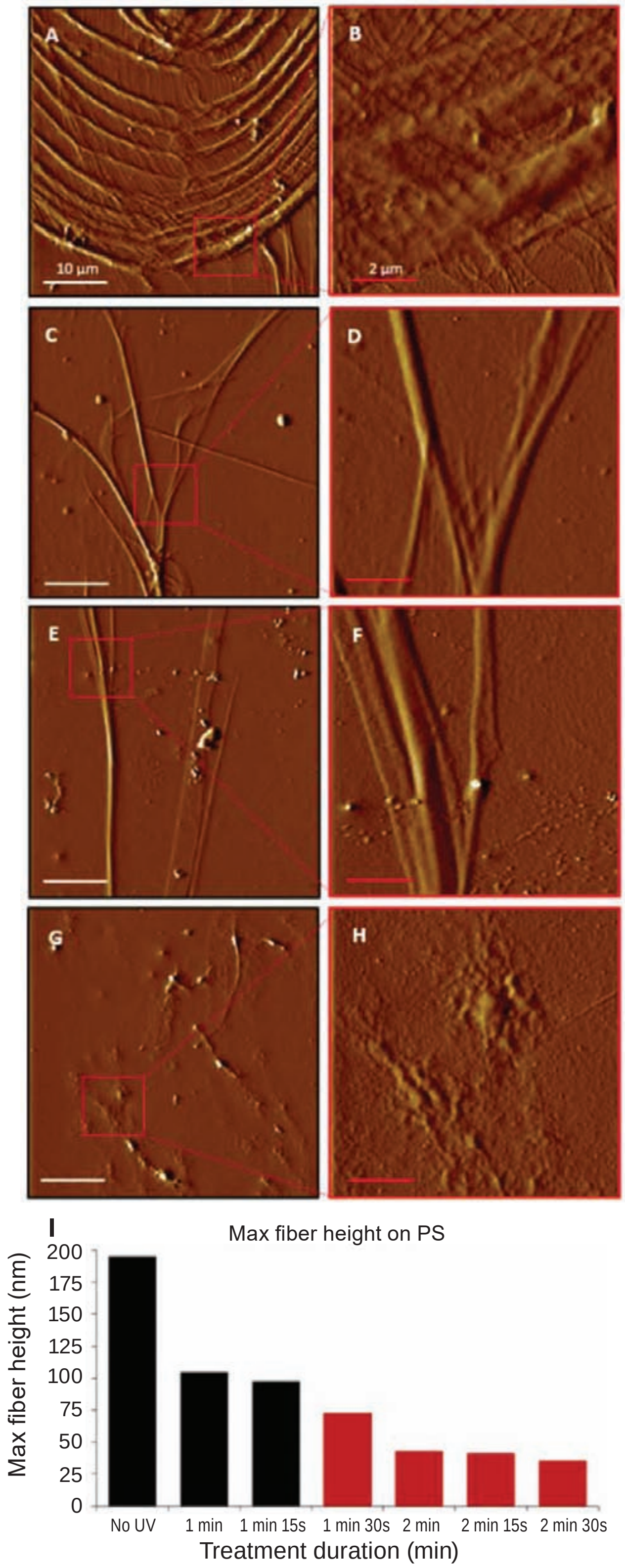

*Fig. 2. Fiber images on PS surfaces obtained using AFM scans post-incubation of 4 mg/ml fibrinogen solution. Deflection images of 50 and 10 μm² shown for UV-ozone exposure durations (**A**, **B**) Control, (**C**, **D**) 1 min, (**E**, **F**) 1 min 30 s, and (**G**, **H**) 2 min with white (10 μm) and red (2 μm) magnification bars. Color ranges for z-scale of images are 0-200 nm. (**I**) Max fiber height analysis as a function of UV-ozone treatment measured using a sectional analysis tool on AFM scans. Bars separated by color for varying surface hydrophilicity*

clay exhibits typical characteristic absorption bands at ~1000, 3417, and 3627 cm^{-1}, which correspond to Si−O and O−H stretching regions, respectively [22]. Once RDP was incorporated into the clay some changes were marked. First, the peak at 1635 cm^{-1}, corresponding to (H−O−H) bending vibrations of free water, was gone following the heating [23]. Furthermore, the Si−O stretching band envelope is impacted by the presence of the RDP, acting as an intercalant as it undergoes self-assembly in the clay galleries, narrowing the Si–O stretching bond with visible shoulder at the 1000-1100 cm^{-1} region [24].

One further point of surface analysis that was researched aimed at describing the true water contact angle of RDP-clay as this would help characterize what occurs at the microscale, and even nanoscale, when fibrinogen meets the clay particles on the materials surface. To accomplish this, RDP-clay aqueous solution was deposited onto a silicon wafer until it fully covered the 1 cm^2 area. Water contact angle measurements were conducted, and the hypothesis that the RDP-clay was hydrophilic was verified. Time-scale images of full wetting of the 100% RDP-clay surface were recorded (Fig. 3, *B*, *C*). Fur-

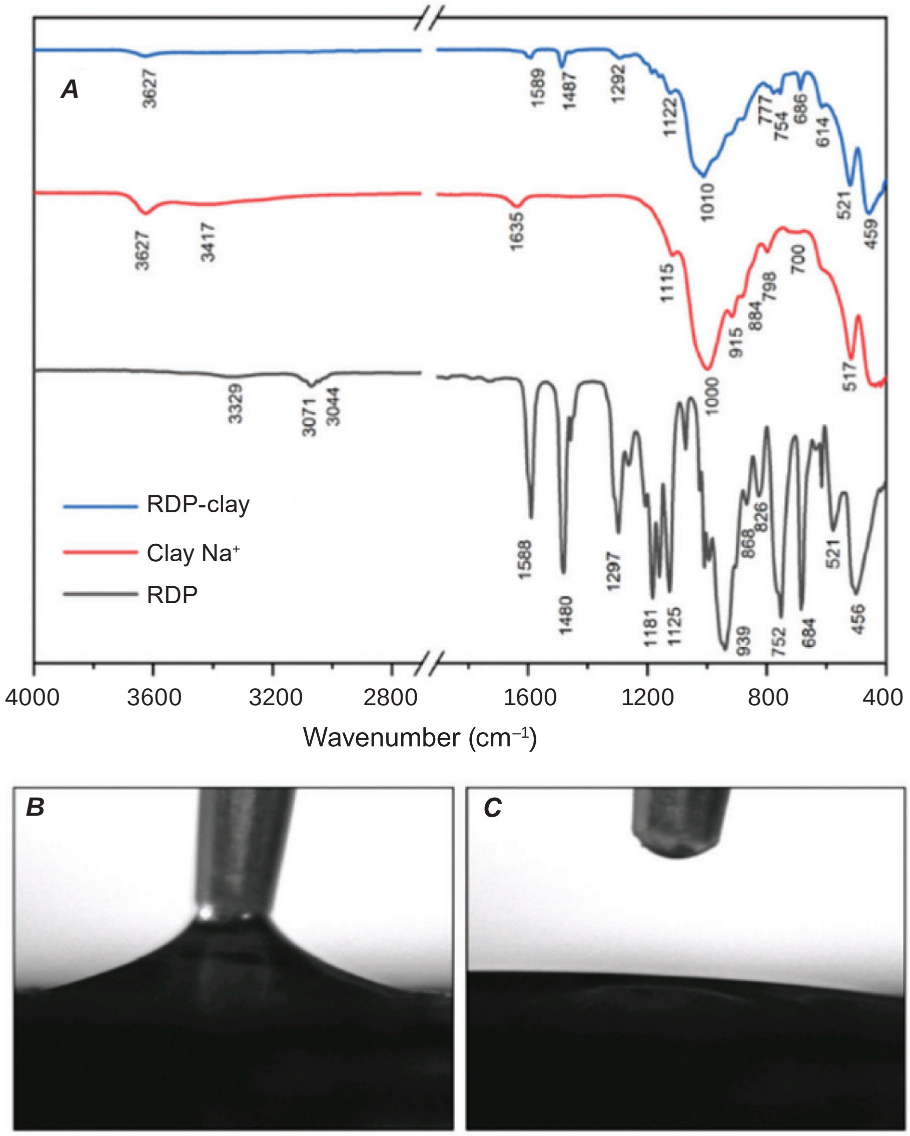

*Fig. 3. Profile of RDP-clay compared to just RDP and pure sodium clay captured using FTIR to show the chemical bonds and functional groups present in individual RDP-clay particles. Images represent 100% RDP-clay surfaces tested with water contact angle image analysis using an optical contact angle meter before (**B**) and after (**C**) applying 5 µl of water*

ther studies aimed to understand how proteins and cells may interact differently on these altered PVA surfaces.

Properties of PVA/RDP-clay substrates. The following investigation aimed at characterizing the surface properties of PVA thin films by analyzing several aspects of the polymer with no changes to its chemistry, or pure PVA, and comparing this to PVA/RDP-clay films following particle inclusion. This was accomplished by incorporating RDP-clay percentages of 0.1, 0.5, 1, 2, 3, 5, 7, and 10 into the PVA material. Following film preparation, AFM imaging was captured to visualize the bulk properties and frictional components. Fig. 4, *A* represents pure PVA, a noticeably flat, featureless surface. Inclusions of RDP-clay were depicted using 2% and 10% (Fig. 4, *B*, *C*), where exfoliated particles and significant increases in surface features can be visualized at 50 μm². Accompanying these features was a drastic increase in frictional forces from the surface, as can be seen from the wavy lines. Such surface properties could be attributed to a change in surface roughness, and data tabulated in Fig. 4, *E* suggests that the increased concentrations of RDP-clay create enhanced roughness of the surface. Average roughness was negligible on control PVA but increased steadily as a linear function of RDP-clay concentration. The concentration of 2% RDP-clay was the median point at around 100 nm and 10% was the largest surface roughness reaching over 200 nm, further highlighting the images of the surface. PVA/RDP-clay surfaces were further characterized by measuring their respective water contact angles in Fig. 4, *D*. It was noted that increasing amounts of RDP-clay were accompanied by significantly decreased contact angles and furthermore, increased

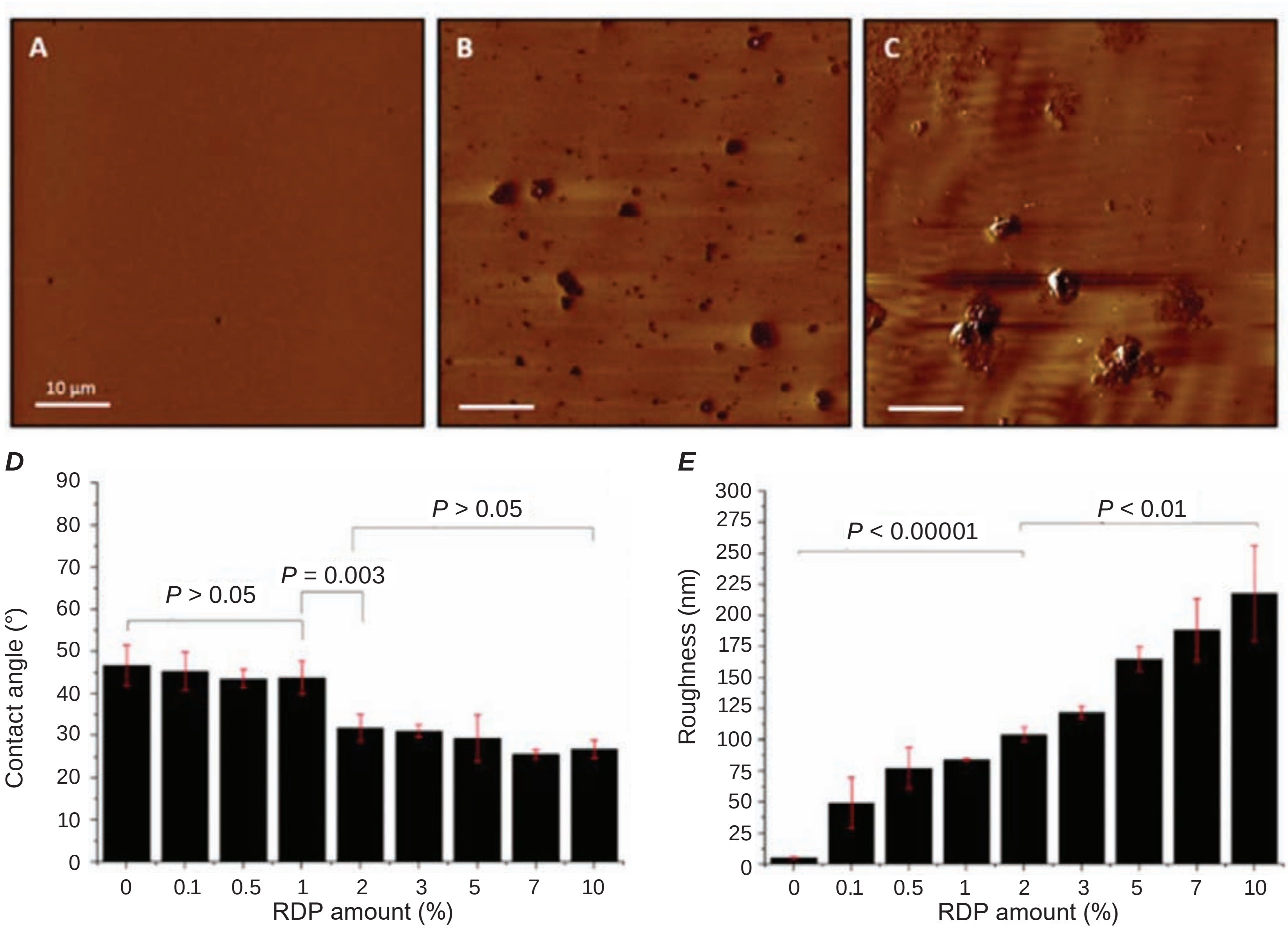

*Fig. 4. Images of PVA/RDP surfaces using AFM scans. Friction images of 50 μm² are shown for RDP-clay inclusions (**A**) Control, (**B**) 2%, and (**C**) 10% with white (10 μm) magnification bars. Color ranges for z-scale of images are 0-190 nm. PVA/RDP-clay thin film surfaces were studied by (**D**) water contact angle analysis and (**E**) surface roughness quantification. Bar graphs represent mean ± SEM*

hydrophilicity. Concentrations of 0-1% slightly reduced the contact angle of PVA with measurements of around 45-50°. Further increasing the concentration to 3-5% led to more significant drops to around 30°. Finally, a minimum range of 25-27° with 7% and 10% RDP-clay. These concentrations brought the contact angle of PVA well below the Berg limit threshold, thereby satisfying the aim and indicating that roughness is a defining factor for the PVA-based materials and allows subsequent classification of the samples. It can also be clearly seen that increasing roughness has an inverse effect on the contact angle and, therefore, on hydrophobicity of the surface.

Influence of surface properties on fiber formation. The next set of experiments aimed to test the PVA/RDP-clay materials' ability to adsorb fibrinogen and reduce surface-initiated fibrillogenesis as a function of increased roughness and hydrophilicity. To accomplish this, the PVA surfaces were incubated in 4 mg/ml fibrinogen solutions. The analysis, and similarly for all other samples, was done by using AFM imaging at scan sizes of 50 and 10 μm^2, respectively. Deflection images for highly detailed structure and height images for the characteristics of fibers were captured and shown in Fig. 5. Evaluation of fiber size was conducted in Fig. 5, *K*, which provides an analysis of maximum fiber height with respect to RDP-clay percentages. The fiber formations were initially analyzed on the control PVA surface with the lowest hydrophilicity, which can be seen in Fig. 5, *A*, *B*. As expected, coarse, fully formed fibers were present on the surface of the polymer and created an elaborate network of outwardly growing, stemming fibers with a maximum height of 153.88 nm. This shows that fibers easily and dynamically polymerize on the surface of the pure PVA sample and that a contact angle of 50.8° is sufficient for fibers to form elaborately on the surface of our polymer, consistent with the Berg limits and our prior studies on PS surfaces. Following the pure PVA control analysis, RDP-clay inclusion was studied. Low percentages of RDP-clay at 0.1 and 0.5% did not significantly deter the growth or structure of the fibrin fibers on these hydrophobic surfaces as the contact angles were very similar to that of the control (images not shown). However, it was noted that there was a reduced maximum height. Fig. 5, *C*, *D* features the initial significant change in fiber formations with the inclusion of 1% RDP-clay, where the fiber networks all but disappeared and maximum fiber height decreased to 70.9 nm. It was noted that some halt in the growth of the fibers occured, but the fibers remained of significant size at this concentration.

The next surfaces analyzed featured increased RDP-clay concentrations past 1%. Starting with 2% concentration, there was a 40% decrease in the contact angle to around 30° and, furthermore, the initial significant decrease in fiber growth was observed (Fig. 5, *E*, *F*). There was no visible network of fiber formation growth like with pure PVA and smaller fibers with maximum heights reducing to about 52 nm. It was also noted that concentrations 3-5% showed similar results (images not shown). The small fibers clearly showed that polymerization on the surface was limited, which suggests that 2-5% RDP-clay concentration acts in accordance with the Berg limits. Next, the additions of 7% and 10% RDP-clay in the PVA material were researched, aiming at describing what occurs when the contact angle is at its lowest point of approximately 26° where the greatest hydrophilicity was displayed. No visible fiber formations were present with these surface properties. At 7% (Fig. 5, *G*, *H*), protein aggregates in the surrounding area appeared to have produced decreased polymerization and were spread out around the visibly immature fiber that did not form or grow enough to produce a coarse fiber structure. This could be attributed to the fact that hydrophilic surfaces do not distort fibrinogen molecules as readily and, therefore, a monolayer incapable of producing fiber formation is present. Looking at the 10% surface (Fig. 5, *I*, *J*), it could be clearly seen that there were no fiber formations whatsoever. There was fibrin deposition with no structural growth or polymerization like with 7%, but much more effectively here. This effectively shows that there is a scattered matte of protein present between the clay particles with no decisive fiber structure.

The effectiveness of this increase on the adsorption of fibrinogen and its tendency to convert into fibrin-like conformations and polymerize due to surface interactions was clearly significantly altered from the incorporation of RDP-clay, which can most likely be attributed to the change in wettability as fibrinogen has a different interaction with hydrophilic surfaces. Previous studies suggest that fibrinogen adsorbs on a different region, namely the hydrophilic αC domains, due to electrostatic attraction or hydrogen bonding, and remains in its folded state on the surface [5, 8]. These results help illustrate that a hydrophilic surface should halt fibrin fiber formation, and it's further shown that this can be achieved through altering the surface properties or surface chemistry of a polymer that previously produced exceptional fibers if the contact angle is reduced appropriately below the Berg limit. Fiber formations were present with concentrations of 2-5% regardless of increased surface hydrophilicity but featuring a significant reduction in the size and structure of the resultant fibers as the RDP-clay percentage increased. Concentrations past 5% featured fully disrupted polymerization, which means an absence in the binding regions required for platelet adhesion. This suggests that these surfaces are not conducive to thrombus formation [25].

Cell adherence and proliferation on PVA/RDP-clay substrates. The next step following our testing of fibrinogen adsorption and fiber formation was to evaluate whether cells adhere and survive on our altered surfaces to ensure cytocompatibility with its changes in surface chemistry. Cell proliferation on PVA substrates containing RDP clay was determined by plating HUVEC-EGFP on PVA thin films containing 0, 1, 3, 5, and 10% RDP clay. Fig. 6, *A* shows the cell doubling time on each type of substrate. The control, 0% RDP clay, was a PVA thin film containing no clay and had a doubling time of 62.9 hours. A one-way ANOVA test was conducted on the data set finding a *P*-value of 0.0521, which was above the 0.05 significance level, indicating that

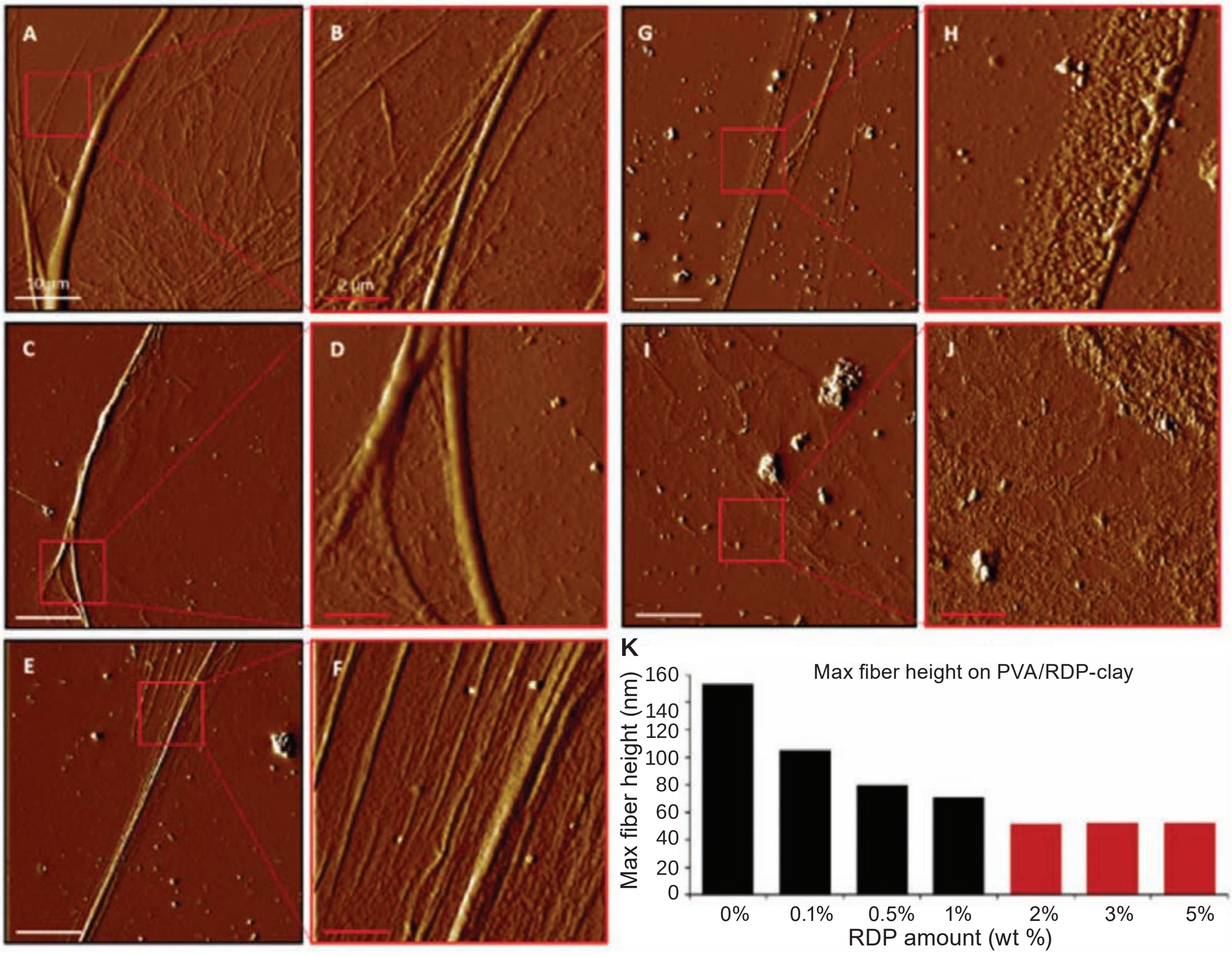

*Fig. 5. Fiber images on PVA/RDP-clay surfaces obtained using AFM scans post-incubation of 4 mg/ml fibrinogen solution. Deflection images of 50 and 10 μm² shown for RDP-clay inclusions (**A**, **B**) Control, (**C**, **D**) 1%, (**E**, **F**) 2%, (**G**, **H**) 7%, and (**I**, **J**) 10% with white (10 μm) and red (2 μm) magnification bars. Color ranges for z-scale of images are 0-150 nm. (**K**) Max fiber height analysis as a function of RDP-clay wt % measured using a sectional analysis tool on AFM scans. Bars separated by color for varying surface hydrophilicity*

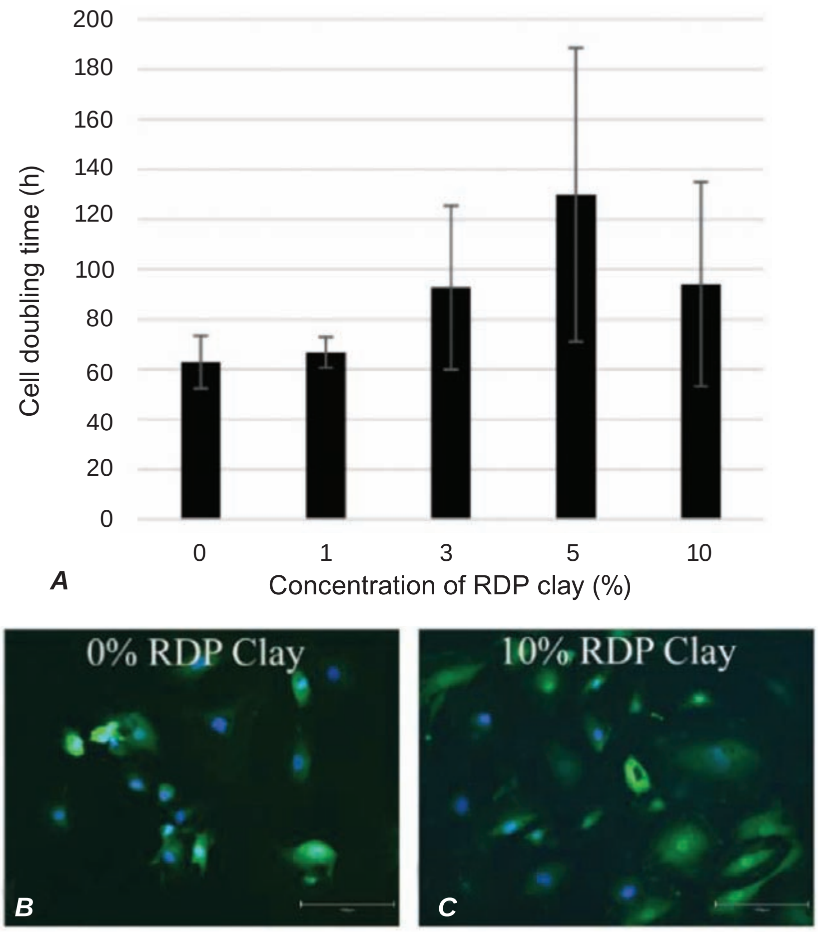

*Fig. 6. (**A**) HUVEC EGFP doubling time on PVA substrates containing 0, 1, 3, 5, and 10% (w/w) RDP clay represented with a mean and standard deviation (N ≥ 5). A one-way ANOVA test was conducted finding P = 0.0521, which does not meet the threshold of significance (α = 0.05) to say there is any difference in doubling time with RDP-clay concentration. Representative fluorescent images (**B** and **C**) of fixed and DAPI stained HUVEC-EGFP were taken on day 5*

none of the samples had a doubling time statistically different from each other. In other words, the inclusion of RDP clay did not change the doubling time compared to the control. Fig. 6, *B* and Fig. 6, *C* show fluorescent images of the cells on day 5 after fixation and DAPI staining. The cells display a spread-out morphology with visible cell-to-cell connections on each type of substrate showing that there is good cell adhesion to the surface. Results from cell studies indicate that there is no significant difference in HUVEC doubling time with the inclusion of RDP-clay into the PVA surface. This suggests that the surfaces are not cytotoxic and, hence, may promote endothelialization. Moreover, this further suggests that PVA/RDP-clay material could be defined as a non-thrombogenic, cytocompatible surface and could be applicable in the development of novel biomaterials.

Conclusion. This study investigates two distinct systems to determine the connections to the Berg limit regarding fibrinogen adsorption and protein aggregation on exposed material surfaces. In both systems, fiber formation is significantly reduced or prevented when the water contact angle is decreased below the critical angle threshold of 50-70°. This suggests that adsorption of fibrinogen can be substantially hindered by altering surface chemistry and, moreover, the absence of conformational changes of adsorbed fibrinogen results in decreased self-assembly. Hence, Berg limit phenomena remain consistent regardless of whether physical or chemical alterations are used. Furthermore, increasing surface hydrophilicity does not appear to negatively affect endothelialization capability. The results convincingly outline a step-by-step procedure, using two different alteration techniques, to counteract surface-induced fibrillogenesis without disrupting endothelialization, an understanding that may help to mitigate thrombotic failure of medical devices.

Conflict of interest. The authors have completed the Unified Conflicts of Interest form at http://ukrbiochemjournal.org/wp-content/uploads/2018/12/coi_disclosure.pdf and declare no conflict of interest.

Funding. We gratefully acknowledge the support of The Louis Morin Charitable Trust and ICL Group.

РОЗРОБКА ПОЛІМЕРНИХ СИСТЕМ, ЗДАТНИХ ЗАПОБІГАТИ ПОВЕРХНЕВО-ІНДУКОВАНОМУ ФІБРИЛОГЕНЕЗУ

A. Hansen[1], A. Sloutski[1], R. Wong[1], Y. Fang[1], L. Stotchel[2], C. Sadasivan[3], M. Rafailovich[1]

[1]Department of Materials Science and Engineering, Stony Brook University, Stony Brook, New York, USA;
[2]Hebrew Academy of Nassau County, Uniondale, New York, USA;
[3]Department of Neurosurgery, Stony Brook University, Stony Brook, New York, USA;
✉e-mail: adam.hansen@stonybrook.edu

Відомо, що використання медичних засобів, які мають полімерні поверхні, що контактують з кровотоком, часто призводить до тромбоутворення. Механізм тромбоутворення залежить, зокрема, від гідрофобної/гідрофільної природи та адгезивних властивостей поверхні, на якій за відсутності тромбіну може відбуватися спонтанно ініційований фібрилогенез. У цій роботі було досліджено зв'язок між «межею Берга» та здатністю полімерних поверхонь продукувати агрегацію фібриногену у волокнисті структури за допомогою двох унікальних систем. Полістирол (PS), добре охарактеризований, стабільний полімер, був спочатку перевірений через його здатність легко надавати гідрофільність за допомогою УФ-озону без додаткових добавок. Однак із метою вивчення біорозкладаного полімеру з більшою фізіологічною значущістю, фокус був переключений на полівініловий спирт (PVA). Для покращення механічних властивостей і підвищення гідрофільності PVA, використано хімічний підхід із додаванням глини, яку функціоналізували дифенілфосфатом резорцину (RDP). Дослідження двох різних систем показали, що адсорбція фібриногену зазнає переходу межі Берга, незалежно від фізичного чи хімічного підходу, і що спостерігається значне зниження поверхневої тромбогенності спричиненої тромбоцитами з контактними кутами нижче цього порогу. Продемонстровано адгезію клітин HUVEC до поверхні PVA-RDP без негативного впливу на проліферацію та здатність до ендотелізації. Таким чином, запропоновано принцип створення нетромбогенних матеріалів шляхом надання поверхні гідрофільності. Цим ефектом можна скористатися для створення полімерів, більш придатних для біомедичних цілей.

Ключові слова: адсорбція фібриногену, утворення волокон, полімерні поверхні, межа Берга, тромбогенність, клітини HUVEC.

References

1. Keohane EM, Smith L, Walenga JM. Rodak's hematology: clinical principles and applications. Elsevier Health Sciences, 2015. 912 p.
2. Mosesson MW. Fibrinogen and fibrin structure and functions. *J Thromb Haemost.* 2005; 3(8): 1894-1904.
3. Galanakis DK, Protopopova A, Li K, Yu Y, Ahmed T, Senzel L, Heslin R, Gouda M, Koo J, Weisel J, Manco-Johnson M, Rafailovich M. Novel characteristics of soluble fibrin: hypercoagulability and acceleration of blood sedimentation rate mediated by its generation of erythrocyte-linked fibers. *Cell Tissue Res.* 2022; 387(3): 479-491.
4. Dempfle CE. The use of soluble fibrin in evaluating the acute and chronic hypercoagulable state. *Thromb Haemost.* 1999; 82(2): 673-683.
5. Zhang L, Casey B, Galanakis DK, Marmorat C, Skoog S, Vorvolakos K, Simon M, Rafailovich MH. The influence of surface chemistry on adsorbed fibrinogen conformation, orientation, fiber formation and platelet adhesion. *Acta Biomater.* 2017; 54: 164-174.
6. Sivaraman B, Latour RA. Delineating the roles of the GPIIb/IIIa and GP-Ib-IX-V platelet receptors in mediating platelet adhesion to adsorbed fibrinogen and albumin. *Biomaterials.* 2011; 32(23): 5365-5370.

7. Chiumiento A, Lamponi S, Barbucci R. Role of fibrinogen conformation in platelet activation. *Biomacromolecules*. 2007; 8(2): 523-531.
8. Koo J, Galanakis D, Liu Y, Ramek A, Fields A, Ba X, Simon M, Rafailovich MH. Control of anti-thrombogenic properties: surface-induced self-assembly of fibrinogen fibers. *Biomacromolecules*. 2012; 13(5): 1259-1268.
9. Murakami D, Kobayashi S, Tanaka M. Interfacial structures and fibrinogen adsorption at blood-compatible poly*mer/water interfaces*. *ACS Biomater Sci Eng*. 2016; 2(12): 2122-2126.
10. Jaffer IH, Fredenburgh JC, Hirsh J, Weitz JI. Medical device-induced thrombosis: what causes it and how can we prevent it? *J Thromb Haemost*. 2015; 13(Suppl 1): S72-S81.
11. Stamboroski S, Joshi A, Noeske PM, Köppen S, Brüggemann D. Principles of fibrinogen fiber assembly *in vitro*. *Macromol Biosci*. 2021; 21(5): e2000412.
12. Kanduč M, Schneck E, Netz RR. Understanding the "Berg limit": the 65° contact angle as the universal adhesion threshold of biomatter. *Phys Chem Chem Phys*. 2024; 26(2): 713-723.
13. Padavan DT, Hamilton AM, Millon LE, Boughner DR, Wan W. Synthesis, characterization and *in vitro* cell compatibility study of a poly(amic acid) graft/cross-linked poly(vinyl alcohol) hydrogel. *Acta Biomater*. 2011; 7(1): 258-267.
14. Zhu G, Zhang F, Jiang P, Ge M. The experimental study of polyvinyl alcohol (PVA) textile material degradation by ozone oxidation process. *J Textile Institute*. 2020; 112(1): 117-122.
15. Gupta S, T G, Basu B, Goswami S, Sinha A. Stiffness- and wettability-dependent myoblast cell compatibility of transparent poly(vinyl alcohol) hydrogels. *J Biomed Mater Res B Appl Biomater*. 2013; 101(2): 346-354.
16. Murakami TN, Fukushima Y, Hirano Y, Tokuoka Y, Takahashi M, Kawashima N. Surface modification of polystyrene and poly(methyl methacrylate) by active oxygen treatment. *Colloids Surf B Biointerfaces*. 2003; 29(2-3): 171-179.
17. Abdulal EA, Khot A, Bailey A, Mehan M, Debies T, Takacs GA. Surface characterization of polystyrene treated with ozone and grafted with poly(acrylic acid). *J Adhes Sci Technol*. 2014; 29(1): 1-11.
18. Guo Y, He S, Yang K, Xue Y, Zuo X, Yu Y, Liu Y, Chang CC, Rafailovich MH. Enhancing the mechanical properties of biodegradable polymer blends using tubular nanoparticle stitching of the interfaces. *ACS Appl Mater Interfaces*. 2016; 8(27): 17565-17573.
19. Xue Y, Yang F, Li J, Zuo X, Pan B, Li M, Quinto L, Mehta J, Stiefel L, Kimmey C, Eshed Y, Zussman E, Simon M, Rafailovich M. Synthesis of an Effective Flame-Retardant Hydrogel for Skin Protection Using Xanthan Gum and Resorcinol Bis(diphenyl phosphate)-Coated Starch. *Biomacromolecules*. 2021; 22(11): 4535-4543.
20. Pack S, Kashiwag T, Cao C, Korach CS, Lewin M, Rafailovich MH. Role of surface interactions in the synergizing polymer/clay flame retardant properties. *Macromolecules*. 2010; 43(12): 5338-5351.
21. Rechendorff K, Hovgaard MB, Foss M, Zhdanov VP, Besenbacher F. Enhancement of protein adsorption induced by surface roughness. *Langmuir*. 2006; 22(26): 10885-10888.
22. Tyagi B, Chudasama CD, Jasra RV. Determination of structural modification in acid activated montmorillonite clay by FT-IR spectroscopy. *Spectrochim Acta A Mol Biomol Spectrosc*. 2006; 64(2): 273-278.
23. Cosultchi A, Cordova I, Valenzuela MA, Acosta DR, Bosch P, Lara VH. Adsorption of crude oil on Na^+-montmorillonite. *Energy Fuels*. 2005; 19(4): 1417-1424.
24. Cole KC. Use of infrared spectroscopy to characterize clay intercalation and exfoliation in polymer nanocomposites. *Macromolecules*. 2008; 41(3): 834-843.
25. Galanakis DK, Protopopova A, Zhang L, Li K, Marmorat C, Scheiner T, Koo J, Savitt AG, Rafailovich M, Weisel J. Fibers generated by plasma Des-AA fibrin monomers and protofibril/fibrinogen clusters bind platelets: clinical and nonclinical implications. *TH Open*. 2021; 5(3): e273-e285.